

This is an Open Access document downloaded from ORCA, Cardiff University's institutional repository: <https://orca.cardiff.ac.uk/id/eprint/107998/>

This is the author's version of a work that was submitted to / accepted for publication.

Citation for final published version:

Kim, Hyunseok, Ren, Dingkun, Farrell, Alan and Huffaker, Diana 2018. Catalyst-free selective-area epitaxy of GaAs nanowires by metal-organic chemical vapor deposition using triethylgallium. *Nanotechnology* 29 (8), 085601. 10.1088/1361-6528/aaa52e

Publishers page: <http://dx.doi.org/10.1088/1361-6528/aaa52e>

Please note:

Changes made as a result of publishing processes such as copy-editing, formatting and page numbers may not be reflected in this version. For the definitive version of this publication, please refer to the published source. You are advised to consult the publisher's version if you wish to cite this paper.

This version is being made available in accordance with publisher policies. See <http://orca.cf.ac.uk/policies.html> for usage policies. Copyright and moral rights for publications made available in ORCA are retained by the copyright holders.



ACCEPTED MANUSCRIPT

# Catalyst-free selective-area epitaxy of GaAs nanowires by metal-organic chemical vapor deposition using triethylgallium

To cite this article before publication: Hyunseok Kim *et al* 2018 *Nanotechnology* in press <https://doi.org/10.1088/1361-6528/aaa52e>

## Manuscript version: Accepted Manuscript

Accepted Manuscript is “the version of the article accepted for publication including all changes made as a result of the peer review process, and which may also include the addition to the article by IOP Publishing of a header, an article ID, a cover sheet and/or an ‘Accepted Manuscript’ watermark, but excluding any other editing, typesetting or other changes made by IOP Publishing and/or its licensors”

This Accepted Manuscript is © 2018 IOP Publishing Ltd.

During the embargo period (the 12 month period from the publication of the Version of Record of this article), the Accepted Manuscript is fully protected by copyright and cannot be reused or reposted elsewhere.

As the Version of Record of this article is going to be / has been published on a subscription basis, this Accepted Manuscript is available for reuse under a CC BY-NC-ND 3.0 licence after the 12 month embargo period.

After the embargo period, everyone is permitted to use copy and redistribute this article for non-commercial purposes only, provided that they adhere to all the terms of the licence <https://creativecommons.org/licenses/by-nc-nd/3.0>

Although reasonable endeavours have been taken to obtain all necessary permissions from third parties to include their copyrighted content within this article, their full citation and copyright line may not be present in this Accepted Manuscript version. Before using any content from this article, please refer to the Version of Record on IOPscience once published for full citation and copyright details, as permissions will likely be required. All third party content is fully copyright protected, unless specifically stated otherwise in the figure caption in the Version of Record.

View the [article online](#) for updates and enhancements.

1  
2  
3 Catalyst-free selective-area epitaxy of GaAs nanowires by metal-  
4  
5  
6 organic chemical vapor deposition using triethylgallium  
7  
8  
9  
10  
11  
12

13 **Hyunseok Kim<sup>1,\*</sup>, Dingkun Ren<sup>1</sup>, Alan C. Farrell<sup>1</sup>, and Diana L. Huffaker<sup>1,2,3</sup>**  
14  
15  
16  
17  
18

19 <sup>1</sup>Department of Electrical Engineering, University of California Los Angeles, Los Angeles, California  
20  
21 90095, United States  
22  
23

24 <sup>2</sup>California Nano-Systems Institute, University of California Los Angeles, Los Angeles, California  
25  
26 90095, United States  
27  
28

29 <sup>3</sup>School of Physics and Astronomy, Cardiff University, Cardiff CF24 3AA, United Kingdom  
30  
31  
32  
33  
34  
35  
36

37 \*E-mail: [hyunseokkim@ucla.edu](mailto:hyunseokkim@ucla.edu)  
38  
39  
40  
41  
42  
43  
44  
45  
46  
47  
48  
49  
50  
51  
52  
53  
54  
55  
56  
57  
58  
59  
60

**ABSTRACT**

We demonstrate catalyst-free growth of GaAs nanowires by selective-area metal-organic chemical vapor deposition (MOCVD) on GaAs and silicon substrates using a triethylgallium (TEGa) precursor. Two-temperature growth of GaAs nanowires – nucleation at low temperature followed by nanowire elongation at high temperature – almost completely suppresses the radial overgrowth of nanowires on GaAs substrates while exhibiting a vertical growth yield of almost 100 %. A 100 % growth yield is also achieved on silicon substrates by terminating Si(111) surfaces by arsenic prior to the nanowire growth and optimizing the growth temperature. Compared with trimethylgallium (TMGa) which has been exclusively employed in the vapor-solid phase growth of GaAs nanowires by MOCVD, the proposed growth technique using TEGa is advantageous because of lower growth temperature and fully suppressed radial overgrowth. It is also known that GaAs grown by TEGa induce less impurity incorporation compared with TMGa, and therefore the proposed method could be a building block for GaAs nanowire-based high-performance optoelectronic and nanoelectronic devices on both III–V and silicon platforms.

**Keywords**

Nanowire, GaAs, MOCVD, catalyst-free, selective-area, TEGa

## 1. INTRODUCTION

Freestanding GaAs nanowires have emerged as promising building blocks for nanoelectronic and nanophotonic devices, such as light-emitting diodes [1], solar cells [2], lasers [3], field-effect transistors [4], and photodetectors [5]. Various growth techniques have been proposed to realize the growth of nanowires with high material quality. Vapor-liquid-solid (VLS) method is the most common method to grow freestanding nanowires, which typically employs Au catalysts as seed particles. However, Au is incorporated in nanowires and substrates during the growth [6], and this is an especially critical problem when grown on Si substrates since deep-level traps are formed in Si by Au impurities [7]. Vapor-solid (VS) method, on the other hand, is a catalyst-free growth technique which does not employ any foreign or self-formed catalysts. Nanowires are grown by the adsorption of vapor-phase atoms and their diffusion on the surfaces in the VS method [8]. This VS growth can arise either on specified positions on the substrates by selective-area epitaxy (SAE) [9, 10] or on random positions of the substrates [11]. The VS SAE technique, which controls the nanowire growth sites by depositing a dielectric film and exposing nanoholes, is particularly useful in the applications requiring precise arrangement of nanowires such as photonic crystal devices [12] and plasmonic devices [13].

Growth of GaAs nanowires by VS SAE has been mostly achieved using metal-organic chemical vapor deposition (MOCVD). Trimethylgallium (TMGa) and triethylgallium (TEGa) are two typical gallium (Ga) sources used for the epitaxy of GaAs thin films; however, for nanowires, TMGa has been a commonly used precursor [9, 14-16] and the use of TEGa is limited [17]. Compared with TMGa, TEGa is known to have much lower decomposition temperature as well as much lower vapor pressure than TMGa, which make TEGa to be more suitable than TMGa when low growth temperature or slow growth rate is required [18, 19]. More importantly, it has been demonstrated that the concentration of carbon impurities in GaAs can be significantly reduced when TEGa is used instead of TMGa, regardless of the group-V precursors [19, 20]. Despite these advantages, there has been no study on GaAs nanowires grown by a SAE technique using TEGa, to the best of our knowledge.

Here, we report on the VS SAE growth of GaAs nanowires by MOCVD using TEGa. The growth on GaAs(111)B substrates shows that the growth temperature and the molar flow rate are two critical factors to achieve high uniformity and high vertical growth yields. A two-temperature growth

1  
2  
3 method – nucleation at a lower temperature followed by nanowire elongation at a higher temperature –  
4  
5 is proposed to completely eliminate radial overgrowth and achieve a growth yield of 100 %. The growth  
6  
7 on Si(111) substrates is also demonstrated to verify the compatibility with silicon-based nanoelectronic  
8  
9 and photonic platforms.  
10

## 11 12 13 14 **2. EXPERIMENTAL SECTION**

15  
16 GaAs nanowires are grown on undoped GaAs(111)B wafers and lightly p-doped (Boron, 10–20  
17  
18  $\Omega$ -cm) Si(111) wafers. First, 20 nm-thick SiO<sub>2</sub> films are deposited on GaAs wafers by electron-beam  
19  
20 evaporation, whereas 20 nm-thick Si<sub>3</sub>N<sub>4</sub> films are deposited on Si wafers by low-pressure chemical  
21  
22 vapor deposition (LPCVD) as growth masks. Then, nanoholes are patterned by electron-beam  
23  
24 lithography, followed by reactive-ion etching (RIE) to expose nanoholes for SAE. CHF<sub>3</sub> and Ar plasma  
25  
26 are used for GaAs substrates, while CHF<sub>3</sub> and O<sub>2</sub> plasma are used for Si substrates in the RIE process  
27  
28 to expose nanoholes. Finally, the wafers are diced into square-shaped 7 × 7 mm<sup>2</sup> size pieces, and the  
29  
30 resist is fully removed by wet etching.  
31

32  
33 The nanowire epitaxy is performed using a low-pressure (60 Torr) vertical MOCVD reactor  
34  
35 (Emcore D-75) which uses hydrogen (H<sub>2</sub>) as a carrier gas. Si samples are cleaned by a 6:1 buffered  
36  
37 oxide etch (BOE) solution for 30 s followed by water rinsing and drying to remove native oxide right  
38  
39 before loading the sample into the reactor. TEGa and tertiarybutylarsine (TBAs) are used as precursors  
40  
41 for all experiments. For the growth on GaAs substrates, the reactor is directly ramped up to 720 °C and  
42  
43 held for 10 min under a TBAs molar flow rate of  $5.33 \times 10^{-5}$  mol/min to perform thermal deoxidation.  
44  
45 Similarly, Si substrates are held at 860 °C for 10 min under H<sub>2</sub> ambient to completely remove native  
46  
47 oxide. Prior to the growth of nanowires on Si substrates, TBAs is supplied with a molar flow rate of  
48  
49  $1.58 \times 10^{-4}$  mol/min for 10 min to form a (111)B-like surface [21]. Detailed growth conditions and  
50  
51 corresponding growth results are discussed below. All growths are terminated by shutting off TEGa  
52  
53 and cooling the reactor down to 300 °C under a TBAs molar flow rate of  $7.40 \times 10^{-5}$  mol/min to prevent  
54  
55 the desorption of nanowires.  
56  
57  
58  
59  
60

1  
2  
3  
4  
5  
6  
7  
8  
9  
10  
11  
12  
13  
14  
15  
16  
17  
18  
19  
20  
21  
22  
23  
24  
25  
26  
27  
28  
29  
30  
31  
32  
33  
34  
35  
36  
37  
38  
39  
40  
41  
42  
43  
44  
45  
46  
47  
48  
49  
50  
51  
52  
53  
54  
55  
56  
57  
58  
59  
60

Optical properties of nanowires are characterized by microphotoluminescence ( $\mu$ PL) measurements. The nanowires are optically pumped using a continuous-wave He-Ne laser operating at 632 nm wavelength. The pump laser is focused using a 50 $\times$  objective lens from the direction normal to the substrate, where the diameter of the laser beam spot on the substrate is approximately 3  $\mu$ m. The emission from nanowires is spectrally resolved by a spectrometer (Acton SP-2500i, Princeton instruments) and a commercial Si photodetector (Model 2151, Newport corporation).

### 3. RESULTS AND DISCUSSION

#### 3.1. GaAs nanowire growth on GaAs(111)B

GaAs nanowires are grown on nanohole arrays with a lattice period of 500 nm and an array size of 50  $\times$  50  $\mu$ m<sup>2</sup> (100  $\times$  100 nanoholes). The diameters of nanoholes are varied from 80 nm to 110 nm to verify the effect of opening sizes on the growth. The samples are grown under various growth temperatures and molar flow rates to study optimized conditions for the nanowire growth. The V/III ratio of TBAs to TEGa is fixed at 30 $\pm$ 5 by adjusting the flow rate of TBAs accordingly.

The nanowire growth is first conducted at 720  $^{\circ}$ C, which is a typical growth temperature in a VS growth mode when TMGa is used [10, 14, 22]. Figure 1 shows GaAs nanowires grown on nanoholes with different diameters. The growth period and the TEGa molar flow rate are 10 min and 2.51  $\times$  10<sup>-6</sup> mol/min, respectively. Although the vertical growth yield is higher than 70 % for all arrays, a non-negligible portion of irregular growths – fat and short nanowires or very short stubs – are clearly observed. The yield is improved at larger mask openings, which can be attributed to the diffusion of adatoms on nanoholes which affects the nucleation inside nanoholes [22, 23].

Since the growth temperature is one of the critical parameters governing the nanowire growth in SAE, GaAs nanowires are grown under various temperatures to compare the growth yield and nanowire morphology. The growth temperatures are varied from 720  $^{\circ}$ C to 620  $^{\circ}$ C, as shown in Figure 2. The growth yield is increased by decreasing the growth temperature from 720  $^{\circ}$ C to 680  $^{\circ}$ C, and reaches 100 % by further decreasing the temperature to 640  $^{\circ}$ C (Figure 2(c)). On the other hand, non-

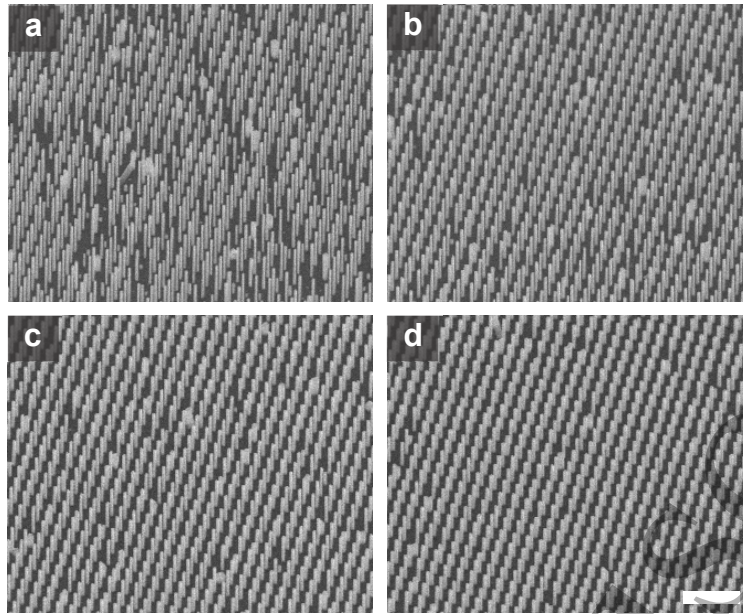


**Figure 1.** 30° tilted SEM images of GaAs nanowires grown at 720 °C for various nanohole opening diameters. (a) 80 nm, (b) 90 nm, (c) 100 nm, (d) 110 nm. The growth yield improves for larger mask openings. Scale bar, 2  $\mu\text{m}$ .

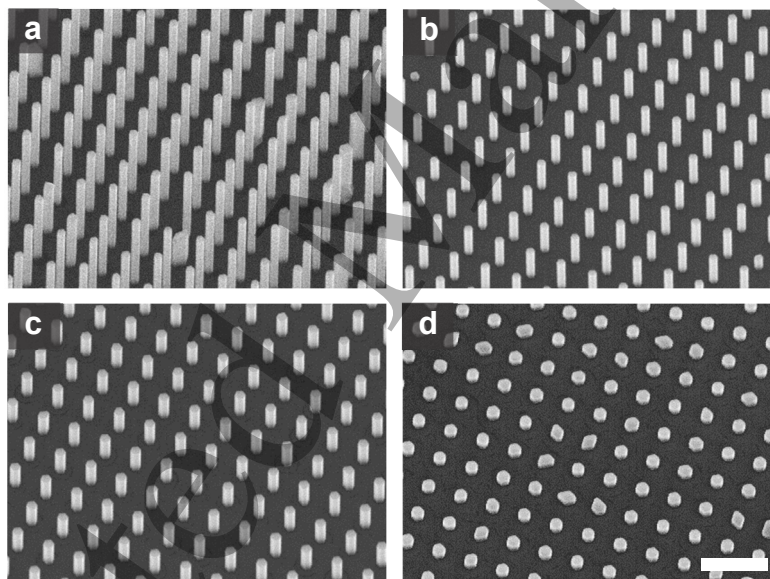


**Figure 2.** 30° tilted SEM images of GaAs nanowires grown under various temperatures. The temperatures are: (a) 720 °C, (b) 680 °C, (c) 640 °C, (d) 620 °C. The diameter of nanohole openings is 90 nm for all arrays. Scale bar, 1  $\mu\text{m}$ .

hexagonal nanowires are observed when the temperature is further decreased to 620 °C. In addition, the nanowires grown at 620 °C show a lower aspect ratio (the ratio of nanowire height to diameter), since nanowires tend to grow radially rather than axially when the growth temperature is decreased [8]. We note that the molar flow rate of TEGa is reduced when the growth temperature is decreased for the nanowires shown in Figure 2. The TEGa molar flow rates are  $2.51 \times 10^{-6}$  mol/min,  $8.03 \times 10^{-7}$



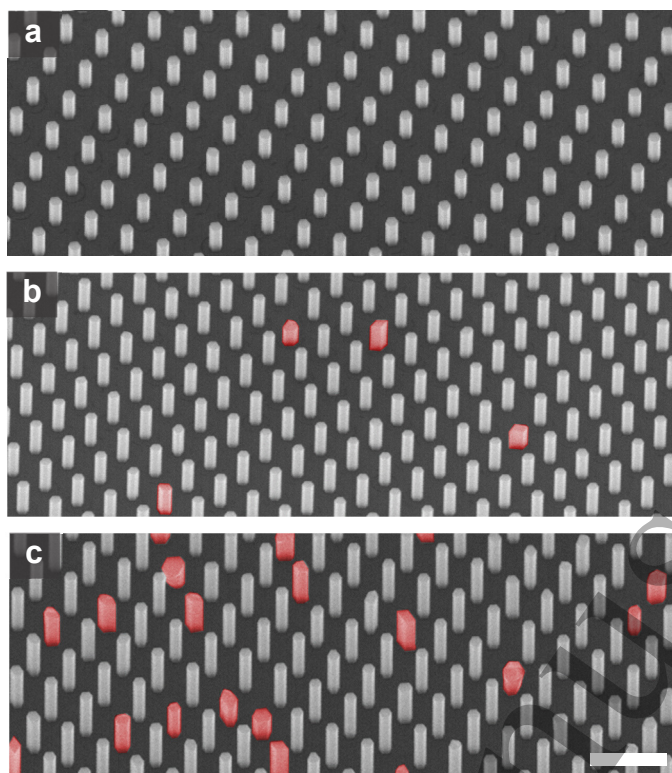


**Figure 3.** 30° tilted SEM images of nanowires grown 640 °C by changing a TEGa molar flow rate. The TEGa flow rate is (a)  $4.01 \times 10^{-7}$  mol/min, (b)  $6.02 \times 10^{-7}$  mol/min, (c)  $8.03 \times 10^{-7}$  mol/min. An increase in non-hexagonal growth is observed as the TEGa molar flow rate is increased. Scale bar, 1  $\mu$ m.

mol/min,  $4.01 \times 10^{-7}$  mol/min, and  $4.01 \times 10^{-7}$  mol/min, corresponding to the temperatures at 720 °C, 680 °C, 640 °C, and 620 °C, respectively. This is because the desorption and evaporation of adatoms are more significant at higher temperatures, and thus the flow of precursors need to be increased to compensate the loss. For instance, the TEGa flow is more than fivefold lower at 640 °C (Figure 2(c)) compared with the flow rate at 720 °C (Figure 2(a)) to realize the growth yield of 100 %. On the other hand, when the TEGa supply is increased by 50 % ( $6.02 \times 10^{-7}$  mol/min) and 100 % ( $8.03 \times 10^{-7}$  mol/min) at 640 °C, an increase in non-hexagonal and polycrystalline growth is observed as shown in Figure 3. It is interesting to note that the optimum growth temperature of 640 °C is significantly lower than the growth temperature of GaAs nanowires using a TMGa source, which is normally around 720 – 750 °C [10, 14, 22]. We ascribe this to the different organic byproducts generated from the cracking of TEGa and TMGa [18, 24], which are adsorbed on the nanowire sidewalls and affect their surface morphology as well as the optimum growth temperature [25]. The differences in the activation energy of TMGa and TEGa could also be one of the reasons for this result [26]. It should be highlighted that

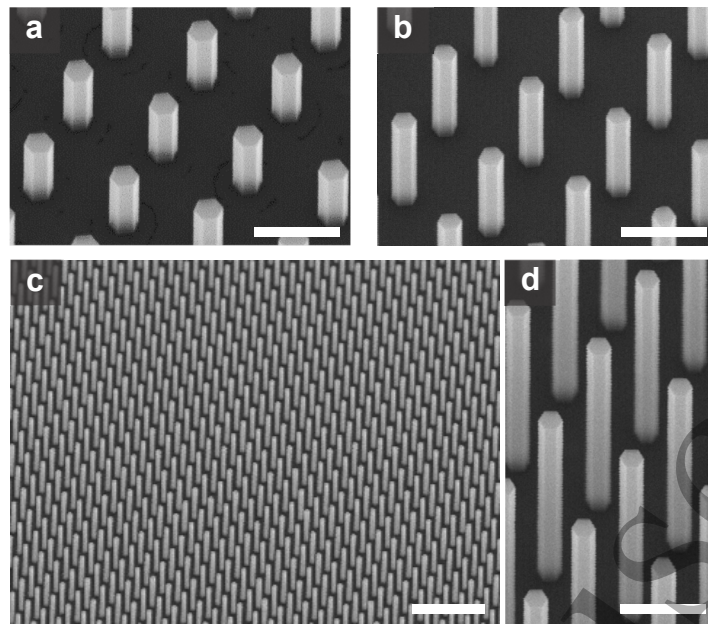


**Figure 4.** Two-temperature growth for high yield and high aspect ratio nanowires. (a) Nanowire growth at 640 °C gives high yield, but low aspect ratio. (b) Growth at 680 °C gives high aspect ratio, but low yield. (c) Nucleation at 640 °C followed by elongation at 680 °C gives high yield and high aspect ratio nanowires. (d) Close-up view of nanowires in (c) All SEM images are taken by tilting the stage by 30°. Scale bars, 500 nm (a, b), 2 μm (c), and 500 nm (d).

such a low growth temperature significantly reduces the diffusion length of atoms in lattices, suggesting that employing TEGa source could enable sharp interfaces when heterostructures are grown in nanowires [10].

Although the growth yield of ~100 % is achieved at 640 °C, as-grown nanowires exhibit non-negligible growth along the radial direction due to the low growth temperature. High-magnification SEM images in Figure 4(a) and Figure 4(b) show that the nanowires grown at 640 °C are fatter and shorter than the nanowires grown at 680 °C. The residual growth along the radial direction could be detrimental for photonic and plasmonic applications requiring a precise control of nanowire dimensions [27, 28]. Furthermore, the lateral overgrowth could lead to the formation of thin shells in nanowire heterostructures, which can act as parasitic paths for carriers and degrade the device performance [29]. To overcome this issue, we implement a two-temperature growth technique. In the two-temperature growth, the nucleation of nanowires is first conducted at 640 °C to ensure a high growth yield, followed by nanowire elongation at higher temperature (680 °C) to suppress radial overgrowth. The nucleation at 640 °C is conducted for 20 min with a TEGa supply of  $4.01 \times 10^{-7}$  mol/min, and the elongation at

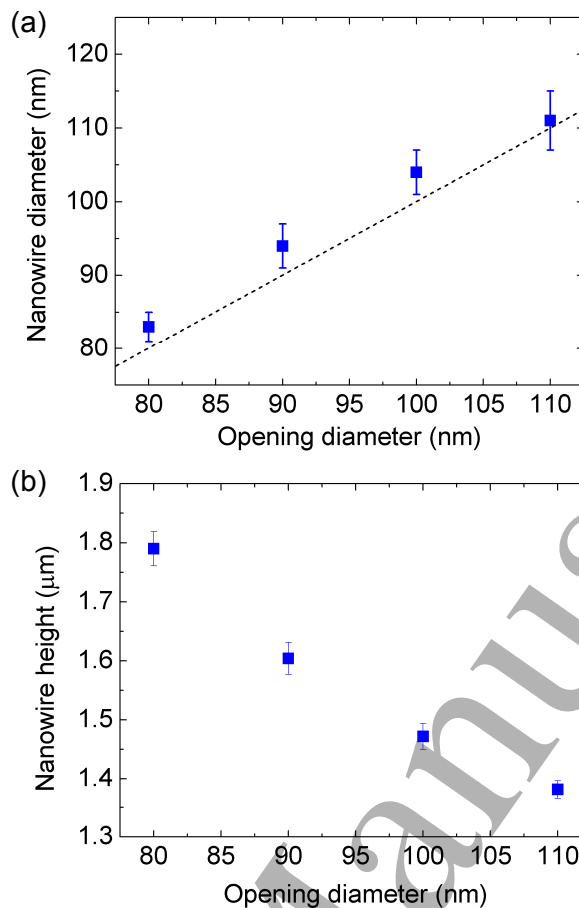


**Figure 5.** (a) Nanowire diameter for various mask opening diameters. Dotted line represents equal opening and nanowire diameter. (b) Nanowire height for various mask opening diameters. Error bars are standard deviation of 50 measured nanowires.

680 °C is conducted for 26 min with a TEGa supply of  $8.03 \times 10^{-7}$  mol/min. As shown in the SEM images in Figure 4(c) and 4(d), the nanowires exhibit 100 % growth yield with an extremely high aspect ratio. The height and diameter of as-grown nanowires are measured to quantitatively analyze the growth rates along the axial and radial directions. It is observed that as the nanohole diameters are increased from 80 nm to 110 nm, the diameters of nanowires are increased from 83 nm to 111 nm as well, as shown in Figure 5(a). The average height of nanowires is decreased from 1.79  $\mu\text{m}$  to 1.38  $\mu\text{m}$  by increasing the nanohole diameter, which is a well-known phenomenon in III–V nanowires grown by SAE techniques [10, 30]. Remarkably, the radial overgrowth is almost negligible (less than 5 nm regardless of the nanohole diameter), and the average vertical to radial growth rate ratio (nanowire height / radial overgrowth) is  $\sim 700$ , which is higher than GaAs nanowires grown by SAE using TMGa [10, 16, 22, 31]. We therefore believe that the proposed two-temperature growth of GaAs nanowires

1  
2  
3 using a TEGa source is a promising approach to enable high-performance nanowire-based devices in  
4  
5 photonic, optoelectronic and electronic applications.  
6  
7

### 8 9 **3.2. GaAs nanowire growth on Si(111)**

10  
11 The growth of GaAs nanowires on Si(111) substrates is also demonstrated using a TEGa source.  
12  
13 Nanohole arrays with a lattice period of 500 nm and an opening diameter of 70 nm is patterned on  
14  
15 Si(111) substrates as a growth template. Compared with III-V substrates, growing vertical nanowires  
16  
17 on Si substrates is not straightforward because GaAs nanowires tend to grow along  $\langle 111 \rangle_B$  directions  
18  
19 whereas Si does not exhibit polarity. Nanowires can therefore grow along any of the four exposed  
20  
21  $\langle 111 \rangle$  directions, which is composed of one vertical  $\langle 111 \rangle$  direction and three angled  $\langle 111 \rangle$  directions.  
22  
23 To control the growth orientation, TBAs is supplied before initiating the nanowire growth to terminate  
24  
25 the exposed Si(111) surface by arsenic and form a (111)B-like surface [21].  
26  
27

28  
29 The GaAs nanowires are grown on Si under various growth temperatures, as shown in Figure  
30  
31 6. TBAs is first supplied for 10 min at the growth temperature, followed by the initiation of nanowire  
32  
33 growth by turning on TEGa. The TEGa flow rate is fixed to  $8.03 \times 10^{-7}$  mol/min regardless of the  
34  
35 growth temperature. As shown in Figure 6(a), the height of nanowires is non-uniform when the growth  
36  
37 temperature is higher than 710 °C. In addition, a significant portion grows as a short stub, which is also  
38  
39 observed from the GaAs nanowires grown on GaAs substrates at high temperatures (Figure 2(a) and  
40  
41 2(b)). The uniformity of nanowires increases by decreasing the temperature, and the vertical growth  
42  
43 yield of nanowires reaches close to 100 % at the growth temperature of 700 °C, as depicted in Figure  
44  
45 6(d). However, at temperatures lower than 700 °C, the growth along angled  $\langle 111 \rangle$  directions starts to  
46  
47 evolve. The portion of angled nanowires and polycrystalline structures is further increased by  
48  
49 decreasing the temperature down to 680 °C. This is attributed to the non-polar nature of Si, whereas  
50  
51 angled nanowires are not observed on GaAs substrates regardless of the growth temperatures.  
52  
53

54  
55 The height and diameter of GaAs nanowires grown at 700 °C is 740 nm and 105 nm,  
56  
57 respectively, which correspond to a vertical to radial growth rate ratio of 21 given that the nanohole  
58  
59 diameter is 70 nm. This is a significantly smaller value than the ratio obtained from GaAs nanowires  
60  
grown on GaAs substrates. This could be due to a strain at the Si/nanowire interfaces, difference in

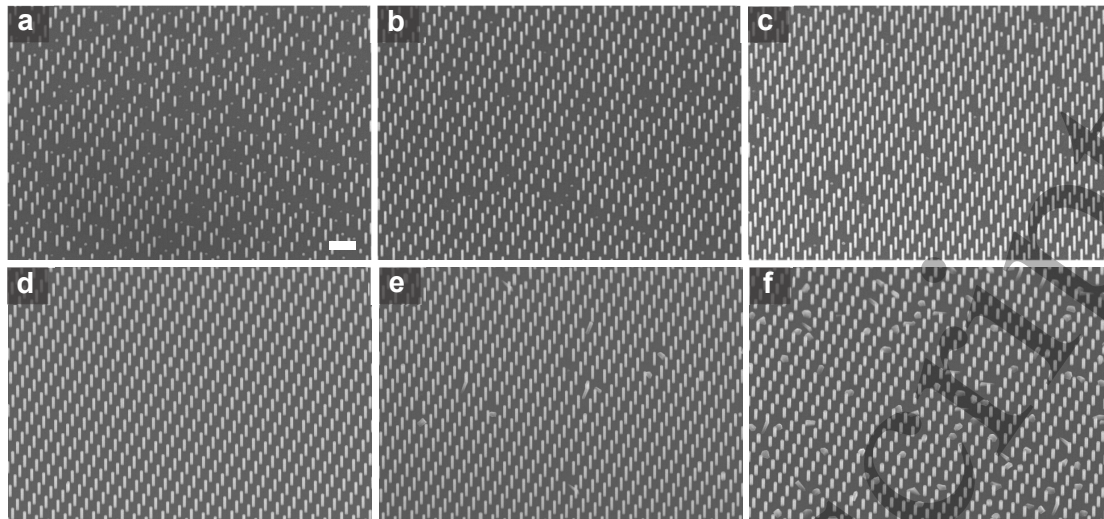


**Figure 6.** 30° tilted SEM images of GaAs nanowires grown on Si under various temperatures. The temperatures are (a) 740 °C, (b) 725 °C, (c) 710 °C, (d) 700 °C, (e) 690 °C, (f) 680 °C. The diameter of nanohole openings is 70 nm for all arrays. Scale bar, 1  $\mu\text{m}$ .

growth temperatures, or dielectric materials of growth masks –  $\text{Si}_3\text{N}_4$  on Si and  $\text{SiO}_2$  on GaAs – which affect the diffusion characteristics of adatoms [32, 33]. However, further study is required to explore this discrepancy.

The optical properties of GaAs nanowires grown on Si are characterized by  $\mu\text{PL}$  measurements at room temperature. For comparison, supplementary nanowire samples are grown on silicon using a TMGa precursor instead of TEGa. The growth temperature is 730 °C when a TMGa source is used, and the nanowires with similar dimensions are chosen for  $\mu\text{PL}$  measurements to properly compare the radiative efficiency. Figure 7 shows the  $\mu\text{PL}$  spectra of GaAs nanowires grown on silicon using TEGa and TMGa at a pump power of 424  $\text{W}/\text{cm}^2$ . Both samples show a dominant peak at 880 nm which corresponds to the bandgap energy of GaAs at room temperature. A relatively long tail is observed at longer wavelengths in these samples, which is typically observed from GaAs nanowires with zinc-blende/wurtzite polytypism [34, 35]. Although the emission from TEGa-grown nanowires is around 20 % stronger than TMGa-grown nanowires, it is unclear whether the difference in the radiative efficiency is stemming from the concentration of carbon impurities. Effects of nanowire surface states, nanowire/substrate interface states, and scattering of carriers from stacking disorders in nanowires need to be considered together with the impurities to evaluate the efficiency. Therefore, further

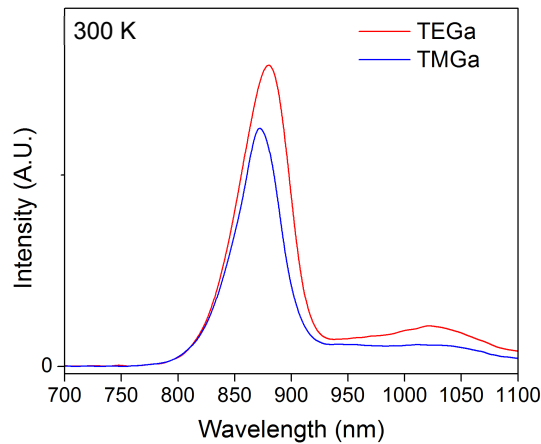


**Figure 7.**  $\mu$ PL spectra of GaAs nanowires on silicon substrates grown using TEGa and TMGa measured at room temperature.

characterization is necessary to elucidate the material properties of GaAs nanowires grown using TEGa and TMGa.

#### 4. CONCLUSION

We have demonstrated a catalyst-free selective-area growth of GaAs nanowires using TEGa. Compared with a commonly-used TMGa source, the TEGa source could be advantageous for controlling the growth rate and lowering the impurity incorporation. A vertical growth yield close to 100 % was achieved on both GaAs and Si substrates by optimizing the growth conditions. A two-temperature growth technique is proposed to fully suppress the radial overgrowth of GaAs nanowires on GaAs substrates while maintaining a high growth yield. The growth of GaAs nanowires on Si implies that the proposed approach can be applied for a monolithic integration of nanowire-based devices on Si platforms.

### Acknowledgements

The authors gratefully acknowledge the generous financial support of this research by AFOSR (through FA9550-15-1-0324), National Science Foundation (through ECCS-1711967 and ECCS-1509801) and Sêr Cymru National Research Network in Advanced Engineering and Materials.

Accepted Manuscript

## References

- [1] Svensson C P T, Mårtensson T, Trägårdh J, Larsson C, Rask M, Hessman D, Samuelson L and Ohlsson J 2008 Monolithic GaAs/InGaP nanowire light emitting diodes on silicon *Nanotechnology* **19** 305201
- [2] Krogstrup P, Jørgensen H I, Heiss M, Demichel O, Holm J V, Aagesen M, Nygard J and i Morral A F 2013 Single-nanowire solar cells beyond the Shockley-Queisser limit *Nature Photonics* **7** 306-10
- [3] Saxena D, Mokkaapati S, Parkinson P, Jiang N, Gao Q, Tan H H and Jagadish C 2013 Optically pumped room-temperature GaAs nanowire lasers *Nature Photonics* **7** 963-8
- [4] Tomioka K, Yoshimura M and Fukui T 2012 A III-V nanowire channel on silicon for high-performance vertical transistors *Nature* **488** 189
- [5] Farrell A C, Senanayake P, Meng X, Hsieh N Y and Huffaker D L 2017 Diode characteristics approaching bulk limits in GaAs nanowire array photodetectors *Nano Letters* **17** 2420-5
- [6] Perea D E, Allen J E, May S J, Wessels B W, Seidman D N and Lauhon L J 2006 Three-dimensional nanoscale composition mapping of semiconductor nanowires *Nano letters* **6** 181-5
- [7] Wang Y, Schmidt V, Senz S and Gösele U 2006 Epitaxial growth of silicon nanowires using an aluminium catalyst *Nature nanotechnology* **1** 186-9
- [8] Shapiro J, Lin A, Huffaker D and Ratsch C 2011 Potential energy surface of In and Ga adatoms above the (111) A and (110) surfaces of a GaAs nanopillar *Physical Review B* **84** 085322
- [9] Noborisaka J, Motohisa J and Fukui T 2005 Catalyst-free growth of GaAs nanowires by selective-area metalorganic vapor-phase epitaxy *Applied Physics Letters* **86** 213102
- [10] Shapiro J, Lin A, Wong P, Scofield A, Tu C, Senanayake P, Mariani G, Liang B and Huffaker D 2010 InGaAs heterostructure formation in catalyst-free GaAs nanopillars by selective-area metal-organic vapor phase epitaxy *Applied Physics Letters* **97** 243102
- [11] Chuang L C, Sedgwick F G, Chen R, Ko W S, Moewe M, Ng K W, Tran T-T D and Chang-Hasnain C 2010 GaAs-based nanoneedle light emitting diode and avalanche photodiode monolithically integrated on a silicon substrate *Nano letters* **11** 385-90
- [12] Kim H, Lee W-J, Farrell A C, Morales J S, Senanayake P N, Prikhodko S V, Ochalski T and Huffaker D L 2017 Monolithic InGaAs nanowire array lasers on silicon-on-insulator operating at room temperature *Nano Letters*
- [13] Senanayake P, Hung C-H, Shapiro J, Lin A, Liang B, Williams B S and Huffaker D 2011 Surface plasmon-enhanced nanopillar photodetectors *Nano letters* **11** 5279-83
- [14] Motohisa J, Noborisaka J, Takeda J, Inari M and Fukui T 2004 Catalyst-free selective-area MOVPE of semiconductor nanowires on (111) B oriented substrates *Journal of crystal growth* **272** 180-5
- [15] Tomioka K, Motohisa J, Hara S, Hiruma K and Fukui T 2010 GaAs/AlGaAs core multishell nanowire-based light-emitting diodes on Si *Nano letters* **10** 1639-44



- 1  
2  
3 [16] Kohashi Y, Sato T, Ikejiri K, Tomioka K, Hara S and Motohisa J 2012 Influence of  
4 growth temperature on growth of InGaAs nanowires in selective-area metal–organic  
5 vapor-phase epitaxy *Journal of Crystal Growth* **338** 47-51  
6  
7 [17] Moewe M, Chuang L C, Crankshaw S, Ng K W and Chang-Hasnain C 2009 Core-  
8 shell InGaAs/GaAs quantum well nanoneedles grown on silicon with silicon-  
9 transparent emission *Optics express* **17** 7831-6  
10  
11 [18] Caneau C, Bhat R, Chang C, Kash K and Koza M 1993 Selective organometallic  
12 vapor phase epitaxy of Ga and In compounds: a comparison of TMI<sub>n</sub> and TEGa  
13 versus TMI<sub>n</sub> and TMGa *Journal of crystal growth* **132** 364-70  
14  
15 [19] Hobson W, Pearton S, Kozuch D and Stavola M 1992 Comparison of gallium and  
16 arsenic precursors for GaAs carbon doping by organometallic vapor phase epitaxy  
17 using CCl<sub>4</sub> *Applied Physics Letters* **60** 3259-61  
18  
19 [20] Hobson W, Harris T, Abernathy C and Pearton S 1991 High quality Al<sub>x</sub>Ga<sub>1-x</sub>As  
20 grown by organometallic vapor phase epitaxy using trimethylamine alane as the  
21 aluminum precursor *Applied physics letters* **58** 77-9  
22  
23 [21] Tomioka K, Motohisa J, Hara S and Fukui T 2008 Control of InAs nanowire growth  
24 directions on Si *Nano letters* **8** 3475-80  
25  
26 [22] Tomioka K, Kobayashi Y, Motohisa J, Hara S and Fukui T 2009 Selective-area  
27 growth of vertically aligned GaAs and GaAs/AlGaAs core–shell nanowires on Si  
28 (111) substrate *Nanotechnology* **20** 145302  
29  
30 [23] Ikejiri K, Sato T, Yoshida H, Hiruma K, Motohisa J, Hara S and Fukui T 2008  
31 Growth characteristics of GaAs nanowires obtained by selective area metal–organic  
32 vapour-phase epitaxy *Nanotechnology* **19** 265604  
33  
34 [24] Larsen C, Li S, Buchan N and Stringfellow G 1989 Mechanisms of GaAs growth  
35 using tertiarybutylarsine and trimethylgallium *Journal of Crystal Growth* **94** 673-82  
36  
37 [25] Sivaram S V, Shin N, Chou L-W and Filler M A 2015 Direct observation of transient  
38 surface species during Ge nanowire growth and their influence on growth stability  
39 *Journal of the American Chemical Society* **137** 9861-9  
40  
41 [26] Salehzadeh O and Watkins S 2011 Control of GaAs nanowire morphology by group  
42 III precursor chemistry *Journal of Crystal Growth* **325** 5-9  
43  
44 [27] Scofield A C, Kim S-H, Shapiro J N, Lin A, Liang B, Scherer A and Huffaker D L  
45 2011 Bottom-up photonic crystal lasers *Nano letters* **11** 5387-90  
46  
47 [28] Kim H, Lee W-J, Farrell A C, Balgarkashi A and Huffaker D L 2017 Telecom-  
48 Wavelength Bottom-up Nanobeam Lasers on Silicon-on-Insulator *Nano Letters* **17**  
49 5244-50  
50  
51 [29] Scofield A, Lin A, Shapiro J, Senanayake P, Mariani G, Haddad M, Liang B and  
52 Huffaker D 2012 Composite axial/core-shell nanopillar light-emitting diodes at 1.3 μ  
53 m *Applied Physics Letters* **101** 053111  
54  
55 [30] Sato T, Motohisa J, Noborisaka J, Hara S and Fukui T 2008 Growth of InGaAs  
56 nanowires by selective-area metalorganic vapor phase epitaxy *Journal of Crystal  
57 Growth* **310** 2359-64  
58  
59 [31] Tatebayashi J, Kako S, Ho J, Ota Y, Iwamoto S and Arakawa Y 2015 Room-  
60 temperature lasing in a single nanowire with quantum dots *Nature Photonics* **9** 501-5

- 1  
2  
3 [32] Jensen L E, Björk M T, Jeppesen S, Persson A I, Ohlsson B J and Samuelson L 2004  
4 Role of surface diffusion in chemical beam epitaxy of InAs nanowires *Nano Letters* **4**  
5 1961-4  
6  
7 [33] Björk M T, Schmid H, Breslin C M, Gignac L and Riel H 2012 InAs nanowire growth  
8 on oxide-masked< 111> silicon *Journal of crystal growth* **344** 31-7  
9  
10 [34] Spirkoska D, Arbiol J, Gustafsson A, Conesa-Boj S, Glas F, Zardo I, Heigoldt M,  
11 Gass M, Bleloch A L and Estrade S 2009 Structural and optical properties of high  
12 quality zinc-blende/wurtzite GaAs nanowire heterostructures *Physical Review B* **80**  
13 245325  
14  
15 [35] Heiss M, Conesa-Boj S, Ren J, Tseng H-H, Gali A, Rudolph A, Uccelli E, Peiró F,  
16 Morante J R and Schuh D 2011 Direct correlation of crystal structure and optical  
17 properties in wurtzite/zinc-blende GaAs nanowire heterostructures *Physical Review B*  
18 **83** 045303  
19  
20  
21  
22  
23  
24  
25  
26  
27  
28  
29  
30  
31  
32  
33  
34  
35  
36  
37  
38  
39  
40  
41  
42  
43  
44  
45  
46  
47  
48  
49  
50  
51  
52  
53  
54  
55  
56  
57  
58  
59  
60